xuv spectra of optical-field-ionized plasmas

E. Fill,[1] S. Borgström,[2] J. Larsson,[2] T. Starczewski,[2] C.-G. Wahlström,[2] and S. Svanberg[2]
[1]*Max-Planck-Institut für Quantenoptik, P.O. Box 1513, D-85740 Garching, Germany*
[2]*Department of Physics, Lund Institute of Technology, P.O. Box 118, S-221 00 Lund, Sweden*
(Received 5 December 1994)

High-power Ti:sapphire laser pulses (150 mJ in 150 fs) were focused into a gas jet of He, N_2, CO_2, O_2, SF_6, or Ar emitted from a pulsed nozzle. The xuv spectra that were generated are reported and analyzed. For all gases the spectra show strong lines corresponding to single-electron transitions. This indicates that the applied intensities of up to 5×10^{16} W/cm^2 readily strip the atoms of all outer electrons, with three-body recombination populating excited levels of the next lower ionization stage. Simulations of the plasma evolution after the laser pulse were performed for helium and nitrogen. In the case of helium, good agreement with the experiment can be obtained for specific initial conditions. For nitrogen, mechanisms other than three-body recombination must be invoked to explain the experimental spectra. Gain measurements were made by comparing longitudinal and transverse spectra. Gains on lines connecting to the ground state or to a quasi-ground-state were not observed, but indications of gains on lines between excited states are reported.

PACS number(s): 52.25.Nr, 52.50.Jm, 42.55.Vc

I. INTRODUCTION

It is well known that an atom can be stripped by many electrons in the field of a high-intensity laser pulse. This effect, known as "optical-field ionization," is one of the most interesting kinds of high-intensity interactions with matter [1–5]. It has been predicted that, depending on whether the beam is linearly or circularly polarized, the electrons are generated with a low or high kinetic energy [4,6]. Optical-field ionization has been suggested as a mechanism for creating favorable conditions for inversions on transitions in the xuv and x-ray regions, taking advantage of the high rate of three-body recombination in an overionized plasma [4–9].

Experiments in which the ions are extracted from the interaction volume have shown [10,11] that the classical barrier suppression model [10,12] quite accurately predicts the threshold intensities $I_{\rm th}$ to produce specific ionic stages. The model results in the following simple formula for the threshold intensity in W/cm^2:

$$I_{\rm th}=\frac{4\times10^9}{q^2}I_q^4 \,. \tag{1}$$

Here q is the charge of the generated ion and I_q is the ionization potential in eV of the ion with charge $(q-1)$.

Table I lists threshold intensities as calculated from Eq. (1) for the generation of various multicharged ions from the gases He, CO_2, N_2, O_2, SF_6, and Ar. At an intensity of 5×10^{16} W/cm^2 it should be possible to strip all electrons from the outermost shell of helium, carbon, nitrogen, and oxygen as well as of sulfur and argon, thus generating bare nuclei of helium, the lithiumlike ionic stage of carbon, nitrogen, and oxygen as well as sodiumlike sulfur and argon. If the ionizing laser pulse is linearly polarized, the temperature of the generated electron cloud should be considerably lower than I_q, resulting in a high rate of three-body recombination. The xuv spectra observed under these conditions should be dominated by single-electron transitions of the ionization stage below that generated by optical-field ionization. The validity of this assertion is experimentally investigated.

TABLE I. Threshold intensities to produce various ions by optical-field ionization according to the barrier suppression model [Eq. (1)].

Ion	Electronic configuration	$I_{\rm th}$ (W/cm^2)
He^+	H-like	1.4×10^{15}
He^{2+}	bare nuclei	8.8×10^{15}
C^{4+}	He-like	4.3×10^{15}
N^{5+}	He-like	1.5×10^{16}
O^{5+}	Li-like	2.3×10^{16}
O^{6+}	He-like	4.0×10^{16}
F^{6+}	Li-like	6.8×10^{16}
F^{7+}	He-like	9.6×10^{16}
S^{6+}	Ne-like	6.7×10^{15}
Ar^{8+}	Ne-like	2.6×10^{16}

II. EXPERIMENT

The experimental arrangement used is shown in Fig. 1. Linearly polarized pulses from a high-power Ti:sapphire laser [13] ($\lambda=794$ nm, pulse duration 150 fs, pulse energy 150 mJ) were focused with a lens of 50 cm focal length to a spot about 50 μm in diameter below a pulsed nozzle, thus generating a peak intensity of about 5×10^{16} W/cm^2. For the majority of the shots a backing pressure of 1.5 bar was used behind the nozzle, resulting in a gas density of about 10^{18} cm^{-3} at a position 250 μm below the nozzle tip, where the laser pulse was focused. The density was measured by an interferometric method [14] modified for application to a pulsed gas jet. A smaller number of shots were made with a backing pressure of 3 bar. How-

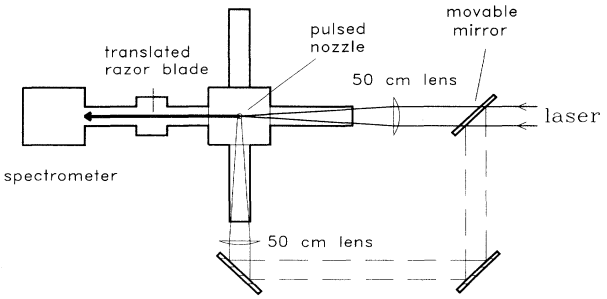

FIG. 1. Experimental arrangement used for recording xuv spectra of optical-field-ionized plasmas.

ever, the changes in the recorded spectra under this condition were insignificant. Due to the difficulty of maintaining at 3 bar a vacuum high enough for safe operation of the photomultiplier used as a detector, a backing pressure of 1.5 bar was chosen for the majority of the shots.

To allow comparison of spectra taken transversally and longitudinally to the direction of the pump laser beam, the beam could be passed around the target chamber by means of a movable mirror and was then focused in a direction 90° to the direction of observation by a similar lens.

Time-integrated xuv spectra were recorded by a 1 m grazing incidence spectrometer equipped with a windowless photomultiplier. Taking advantage of the 10 Hz shot rate of the laser each data point of the spectrum was averaged over 50 shots, rejecting shots with energies deviating more than $\pm 15\%$ from the nominal value.

III. RESULTS

Quite generally, it was found that the generation of high ionic charges depended critically on the adjustment of the focus into the gas jet. If the beam was not well focused below the nozzle tip, only odd harmonics of the laser frequency and lines from low ionization stages could be detected. With a well focused beam, however, reproducible spectra of multiply ionized species were obtained.

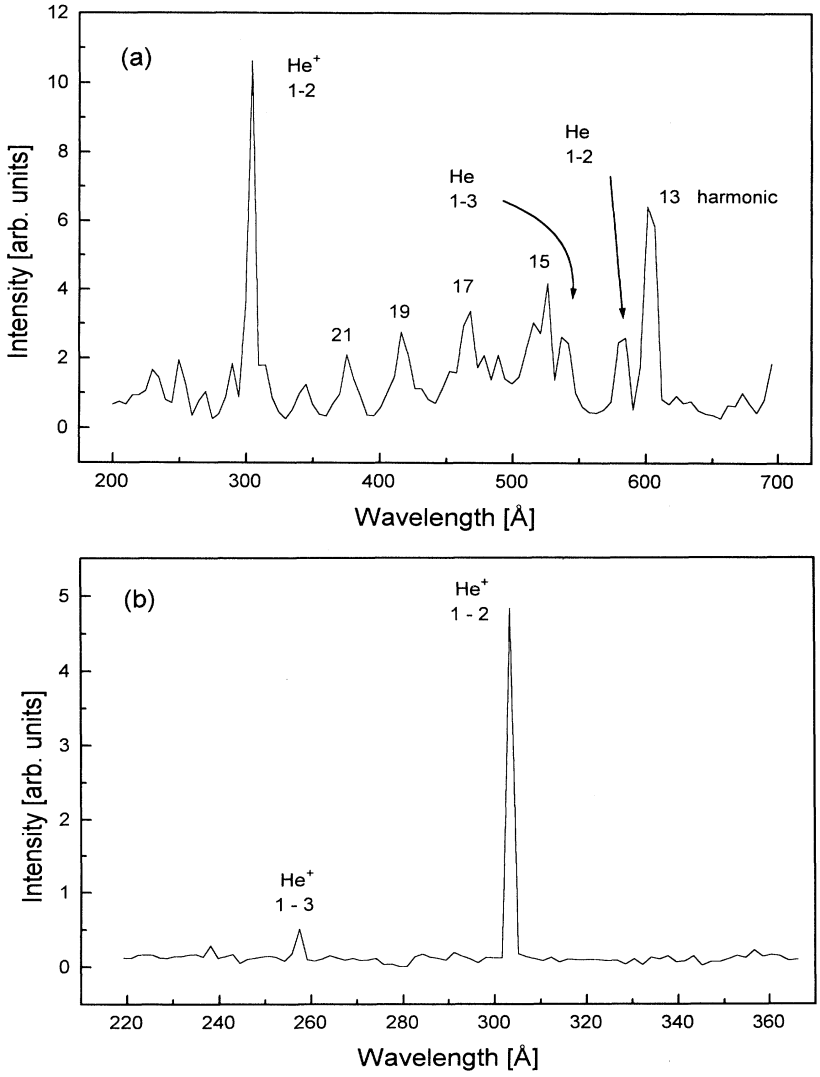

FIG. 2. Longitudinal spectra of helium. (a) Low dispersion spectrum showing 1-2 and 1-3 lines of neutral helium, as well as harmonics and hydrogenic resonance lines. (b) Spectrum with higher dispersion in the region of hydrogenic resonance lines.

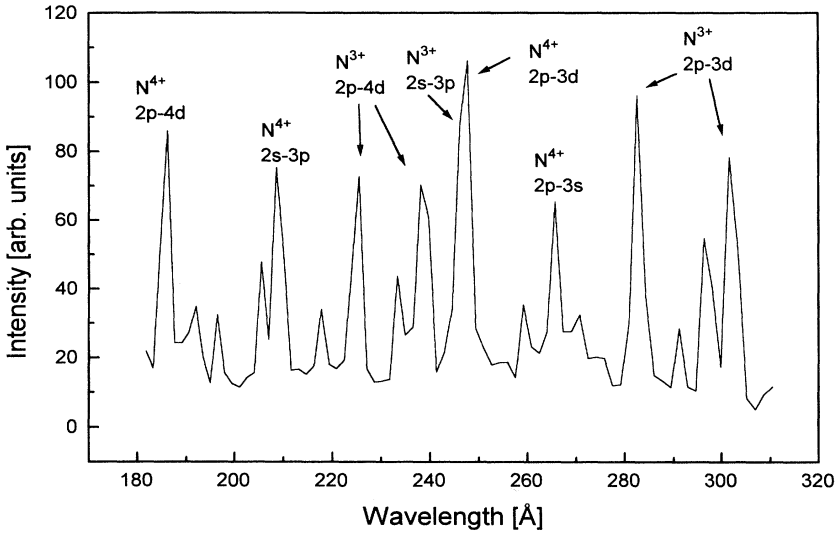

FIG. 3. Transverse spectrum of nitrogen in the region of lithiumlike resonance lines showing lithiumlike and berylliumlike lines (N^{4+} and N^{3+}).

A. xuv spectra

The identification of the spectral lines was performed using standard wavelength tables [15,16]. For lithiumlike and sodiumlike lines the wavelengths calculated by Lindgard and Nielsen [17] were found helpful.

Longitudinal spectra of helium are shown in Figs. 2(a) and 2(b). As expected from the discussion above, the spectrum is dominated by the hydrogenic lines. Most striking is the strong Lyman-α emission in relation to Lyman-β, strongly suggesting gain on the Lyman-α transition. It turned out, however, that the transverse spectra looked quite similar, and, as will be discussed below, different reasons are responsible for this feature.

Figure 3 shows a transverse spectrum of nitrogen in the spectral region 180–310 Å. The spectrum is dominated by lithiumlike and berylliumlike lines, the lithiumlike $2p$-$3d$ line being the strongest one. However, the $2p$-$4d$ line has almost the same intensity. This finding is in strong contrast to the observation in helium and suggests that the plasma parameters for helium and nitrogen may be quite different.

The spectra obtained from the gases CO_2, O_2, SF_6, and Ar are shown in Figs. 4–7. The spectrum obtained from CO_2 (Fig. 4) shows that in carbon the situation is quite similar to the case of nitrogen. Again, the $2p$-$4d$ resonance line is almost as strong as the $2p$-$3d$ line.

The oxygen spectrum (Fig. 5) has an abundance of lines, with ionization stages lower than lithiumlike contributing most of these. It is clear that the lithiumlike stage could only marginally be generated, in accordance with the fact that the intensity required to generate lithiumlike oxygen is close to the maximum intensity of our experiment (see Table I).

The spectrum obtained from SF_6 (Fig. 6) shows Na-like sulfur transitions, indicating that Ne-like sulfur was readily generated. Lines of low ionization stages of fluorine are also observed. Lithiumlike fluorine lines are

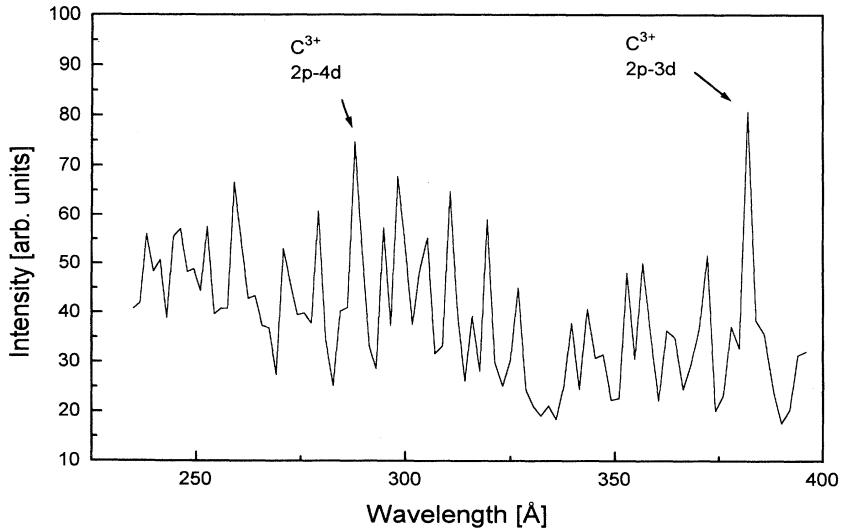

FIG. 4. Transverse spectrum of CO_2 in the region of lithiumlike carbon resonance lines.

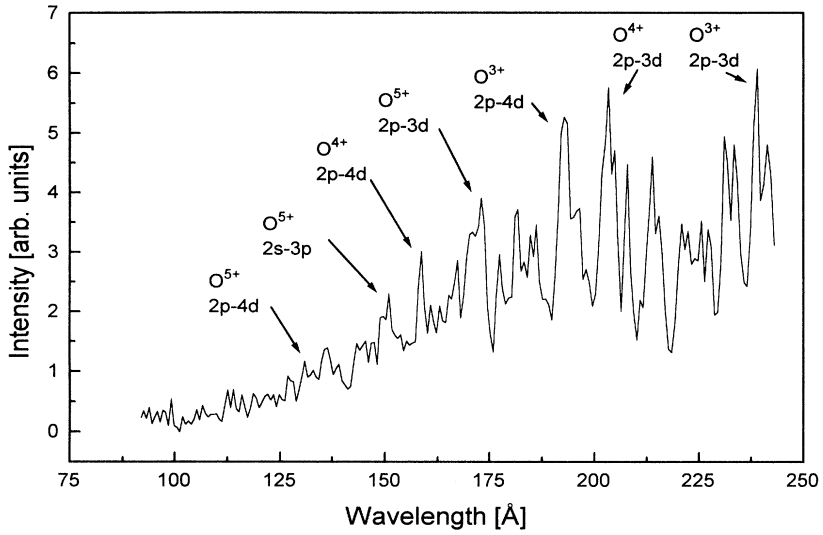

FIG. 5. Transverse spectrum of oxygen in region of lithiumlike resonance lines.

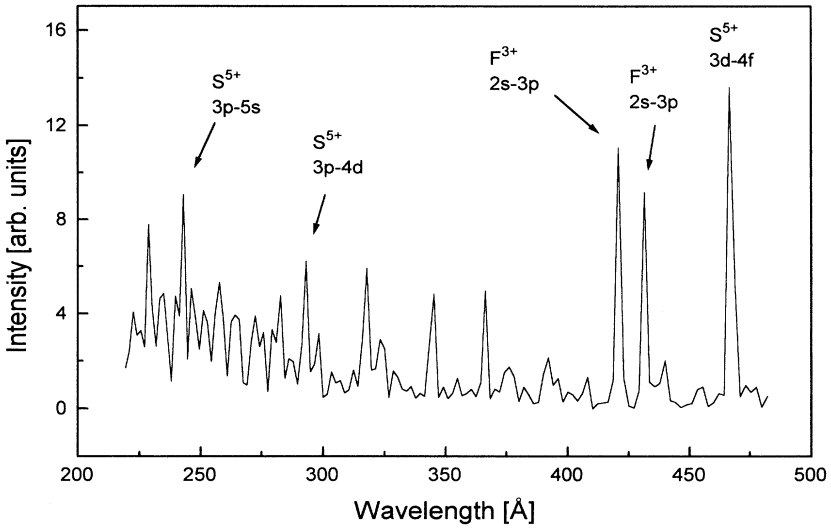

FIG. 6. Transverse spectrum of SF_6 in region of sodiumlike sulfur resonance lines. Lines of sodiumlike sulfur (S^{5+}) and of carbonlike fluorine (F^{3+}) are prominent in the spectrum. Note that some of the lines have not been identified.

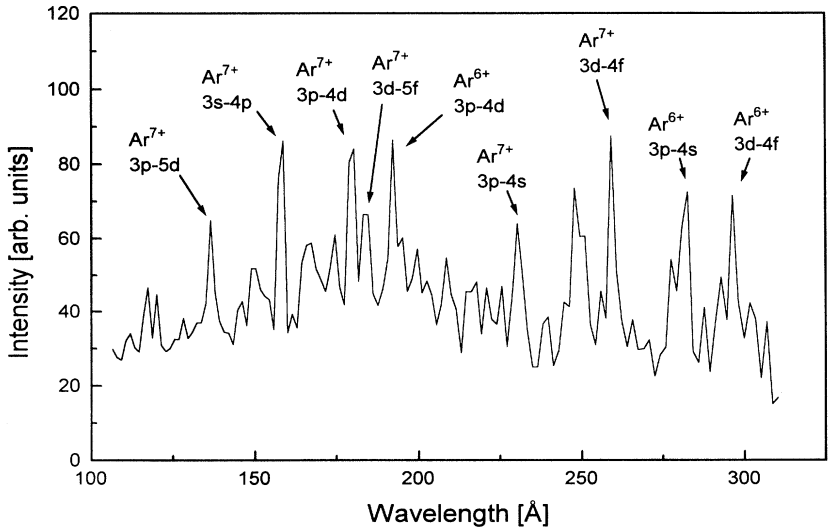

FIG. 7. Transverse spectrum of argon in region of sodiumlike resonance lines, showing sodiumlike and magnesiumlike lines (Ar^{7+} and Ar^{6+}).

not seen, in accordance with the prediction of Eq. (1) that the threshold intensity to generate lithiumlike fluorine is too high. Note that several of the lines could not be identified.

In the argon spectrum (Fig. 7) Na-like and Mg-like lines contribute the majority of the lines. The Na-like 3-4 resonance lines show the highest intensities, but Na-like 3-5 lines are relatively strong.

B. Intensity dependence

For several lines the dependence of the emission on laser intensity was determined. For this purpose the spectrometer was set to the respective wavelength and the emission was recorded while the energy of the laser pulse was continuously varied. Each data point was averaged over 20 shots. For all of the lines investigated a nonlinear increase of the emission with laser intensity was observed.

It must be checked if such an increase can be explained with a volume effect. Two analytical cases may be considered. (a) For a Gaussian beam of peak intensity I_0 in an infinite medium the volume in which the intensity is greater than $I_{\rm th}$ is given by [11]

$$V=\pi z_R w_0^2[\tfrac{4}{3}c+\tfrac{2}{9}c^3-\tfrac{4}{3}\tan^{-1}(c)]\ , \tag{2}$$

where $2w_0$ is the focal spot, z_R is the Rayleigh range of the focus, and $c=(I_0/I_{\rm th}-1)^{1/2}$. (b) If the focal region is limited to a length $2L$ then the volume in which the intensity exceeds $I_{\rm th}$ is

$$V=\pi L w_0^2 \ln(I_0/I_{\rm th})\ . \tag{3}$$

In the experiment $2z_R \approx 1$ mm. The interaction length $2L$ is limited by the diameter of the gas jet, which is about 500 μm. Since there is no sharp boundary of the medium, an experimental intensity variation caused by a volume effect should exhibit a dependence in between the two limiting cases. As shown in Fig. 8 for the N^{4+} $2p$-$3d$ emission this is indeed observed. Similar behavior was shown by several other lines including He^+ Lyman-α. Thus it cannot be excluded that a volume effect is responsible for the observed nonlinear increase in intensity.

C. Spatial distribution

A number of runs were made to determine the spatial region from which the plasma emission occurred. For this purpose, a razor blade was inserted into the beam halfway between the nozzle and the spectrometer entrance slit. Recording the intensity of a particular line while translating the razor blade into the beam yielded curves as shown in Figs. 9(a) and 9(b) for He^+ Lyman-α and N^{4+} $2p$-$3d$. These data are evaluated by differentiating with respect to the spatial position of the razor blade and performing an Abel inversion [18]. The emission is found to originate from a region about 140 μm in diameter for He^+ Lyman-α and about 125 μm in diameter for N^{4+} $2p$-$3d$. This finding is explained by the expansion of the optical-field-induced ionization channel [19], which occurs at a velocity proportional to $(qT_e/m)^{1/2}$, where T_e is the electron temperature and m the ion mass. Using an electron temperature of 40 eV for helium and 20 eV for nitrogen (see below) the simulations described in the next section predict expansion velocities of 3.7×10^6 cm/s for helium and 2.1×10^6 cm/s for nitrogen. (These velocities apply to the $1/e$ radius of the Gaussian density distribution in the self-similar expansion.) Thus the observed emission region corresponds roughly to the expansion during 1–2 ns.

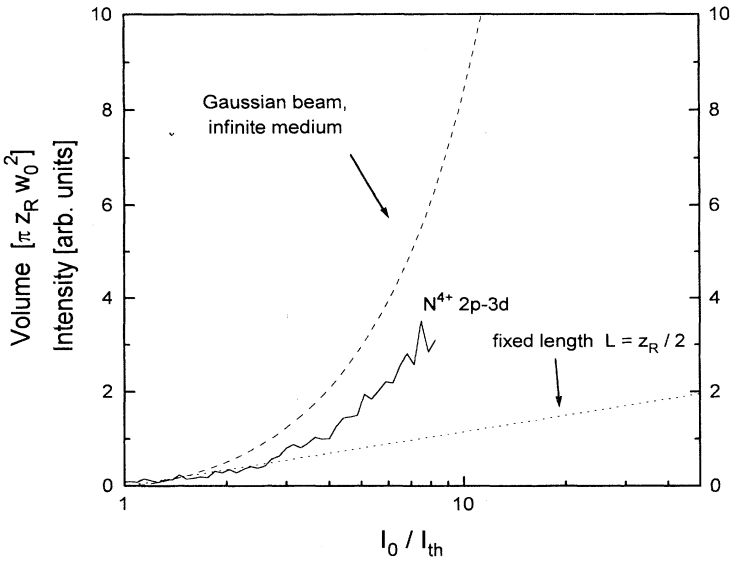

FIG. 8. Dependence of N^{4+} $2p$-$3d$ emission on laser intensity. Two different curves expected from a volume effect are also shown. Dashed line: volume of a gaussian beam the peak intensity of which exceeds a threshold intensity by a factor as given on the abscissa [Eq. (2)]. Dotted line: Same but with length L fixed to $z_R/2$ [Eq. (3); z_R = Rayleigh range].

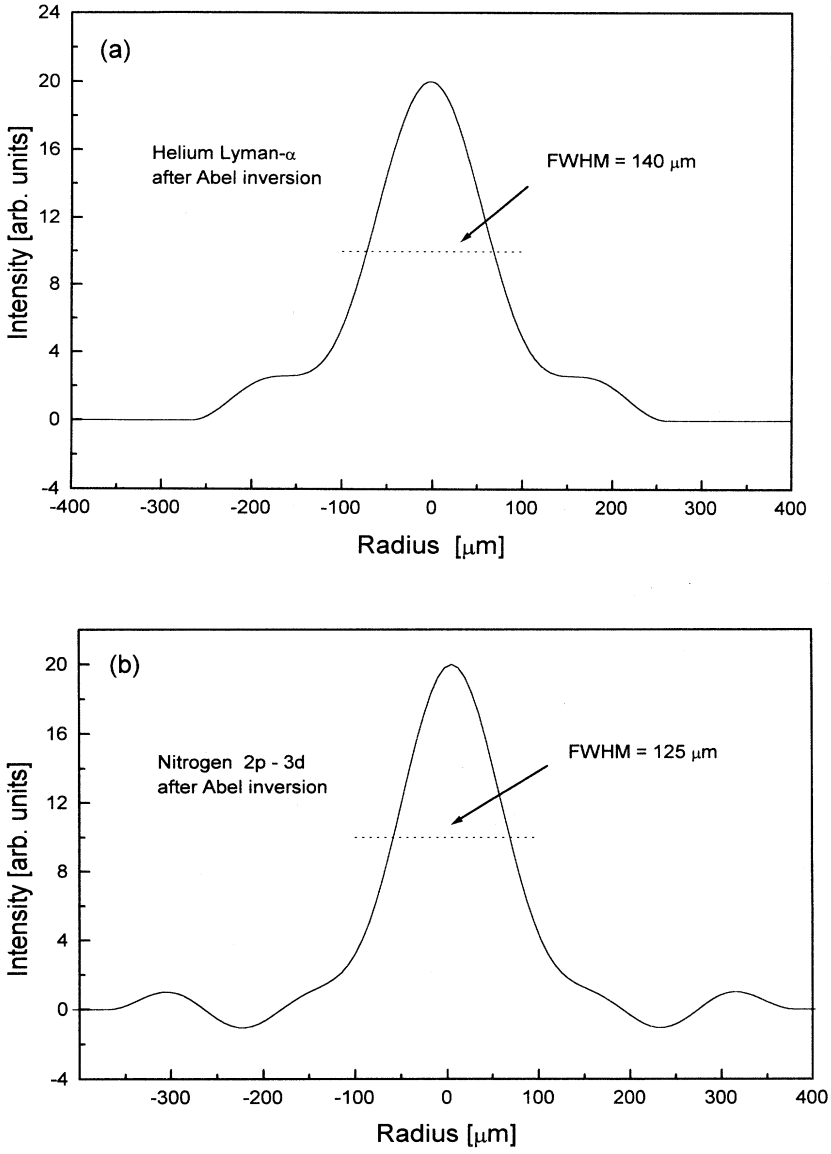

FIG. 9. Spatial extent of region emitting (a) He^+ Lyman-α and (b) N^{4+} $2p$-$3d$ lines. The curves are generated by differentiation and Abel inversion of data obtained by scanning a razor blade through the xuv beam (see Fig. 1).

IV. ANALYSIS AND DISCUSSION

A special feature of the recorded spectra is the striking dissimilarity between the helium spectra and the spectra of the other gases, with respect to the relative intensities of the lines originating from upper levels with different quantum numbers.

A partial explanation for this observation can be derived from the different electron temperatures in the two cases if the initial electron temperature is assumed to be due to above threshold ionization (ATI) heating [4,12,20]. Recent Thomson scattering measurements of the electron temperature in optical-field-ionized plasmas confirm this assumption [21,22]. By taking the temporal and spatial average over the laser pulse [12] a temperature of 40 eV is estimated for helium, whereas the corresponding temperature for nitrogen is 20 eV. The lower electron temperature for nitrogen results from the fact that in nitrogen the main part of the electrons comes from comparatively low ionization stages. The situation is similar for the other gases used in the present experiments.

Note that in the case of helium the electron temperature is close to the ionization potential of hydrogenic helium (54.4 eV), whereas for nitrogen it is considerably below the ionization potential of lithiumlike nitrogen (97.4 eV). Thus the recombination rate should be low in helium, whereas in nitrogen (and for the other gases of our experiments) it should be high.

To corroborate the above arguments, simulations of the plasma evolution after the ionizing laser pulse were performed, concentrating on helium and nitrogen. For the simulations the plasma was assumed to be in a specified initial state after the laser pulse and then ionic level populations were calculated by means of a collisional radiative computer code. Hydrodynamic motion and adiabatic cooling were modeled by means of the self-

similar solution of London and Rosen [23]. The time-integrated emission on the various transitions was then calculated for transverse and longitudinal spectra. Opacity was taken into account with quasistatic ion broadening being assumed to be the main broadening mechanism for the He^+ Lyman lines. For nitrogen, Doppler-broadened lines were assumed with an initial ion temperature given by conservation of momentum. To calculate transverse spectra the hydrodynamic expansion of the plasma column was taken into account. Because of the low ion density and the relatively large linewidths, opacity had little effect for helium. For nitrogen, however, the strongest lines were somewhat reduced in intensity by self-absorption.

A. Helium

In the case of helium the main feature to be reproduced by the simulations is the high Lyman-α to Lyman-β ratio observed in the spectra. Using the "standard" initial conditions $T_e = 40$ eV (as estimated from ATI heating), $N_e = 2\times10^{18}$ cm^{-3} (as obtained from the gas density), and assuming that immediately after the laser pulse the density of hydrogenic ions in the ground state is zero, one obtains a Lyman-α to Lyman-β ratio significantly different from the experimental one.

The simulated spectrum is brought into agreement with the experimental one if the initial conditions are modified. A first possibility is to maintain the standard initial conditions for the electron temperature and density, but assume that a certain amount of the initial ions are in the hydrogenic ground state (rather than being bare nuclei). If one compares the relative magnitude of recombination and excitation rates it appears that even at a relatively low population of the He^+ ground state the excited states are predominantly populated by excitation from the ground state and recombination only slightly effects the level populations. The reason for this is the low recombination rate due to the high electron temperature. The low intensity of the Lyman-β line results from a small excitation rate of the $n = 3$ level since the electron density is considerably below that required for local thermal equilibrium (LTE).

The effect of varying the initial population in the hydrogenic helium ground state is demonstrated in the diagram shown in Fig. 10, which displays the resulting Lyman-α to Lyman-β ratio. It is obvious that a hydrogenic helium ground state population of only 0.7% of the total initial ion population reproduces the experimentally observed line ratio.

A different assumption for the initial conditions also results in a Lyman-α to Lyman-β ratio as experimentally observed: For this set of conditions the initial population in the hydrogenic helium ground state is assumed to be zero but the initial electron temperature is reduced far below that calculated from ATI heating. Now the Lyman-β emission is quenched by electron-collisional deexcitation of the $n = 3$ level to the $n = 2$ level. As seen in Fig. 11, the experimental line ratio is matched to the theoretical one at an electron temperature of about 6 eV.

The fact that the simulated spectra can be brought into accord with the experimental ones by two different assumptions for the initial conditions complicates the interpretation of the helium results. In view of the experimental verification of ATI heating as the mechanism determining the electron temperature in optical-field-ionized helium [21,22], it seems that the first scenario, in which the helium spectra are explained in terms of excitation from the hydrogenic ground state, is the more likely one.

B. Nitrogen

Like the computer-generated spectra for helium, those for nitrogen are not in accord with the experimental ones if standard initial conditions, i.e., an electron temperature of 20 eV (as determined by ATI heating), an electron density of 10^{19} cm^{-3} (as derived from the density), and zero population in any of the lithiumlike ground states are assumed. Figure 12 shows a transverse spectrum obtained by the simulation. The main difference in the spectrum is

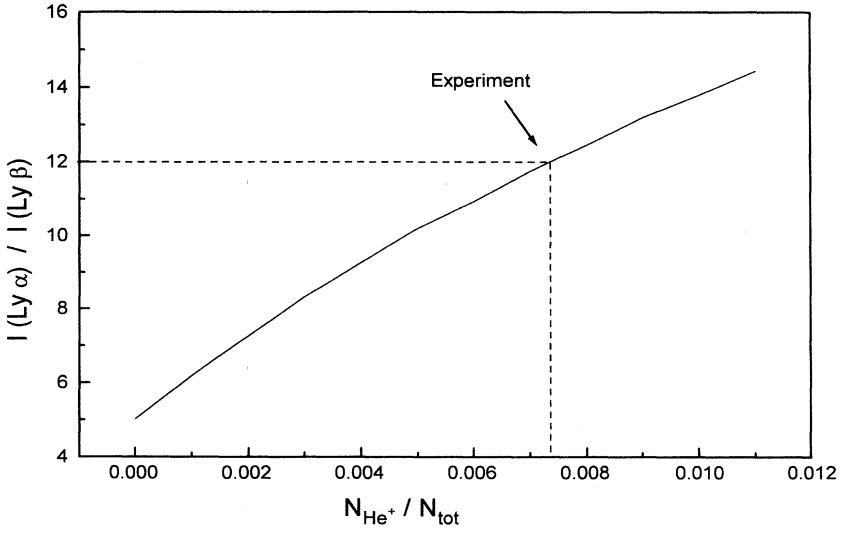

FIG. 10. Result of a simulation of the plasma evolution after optical-field ionization: helium. Effect of varying the initial hydrogenic ground state population on He^+ Lyman-α to Lyman-β ratio. N_{tot} = total initial ion density. Experimental line ratio is indicated.

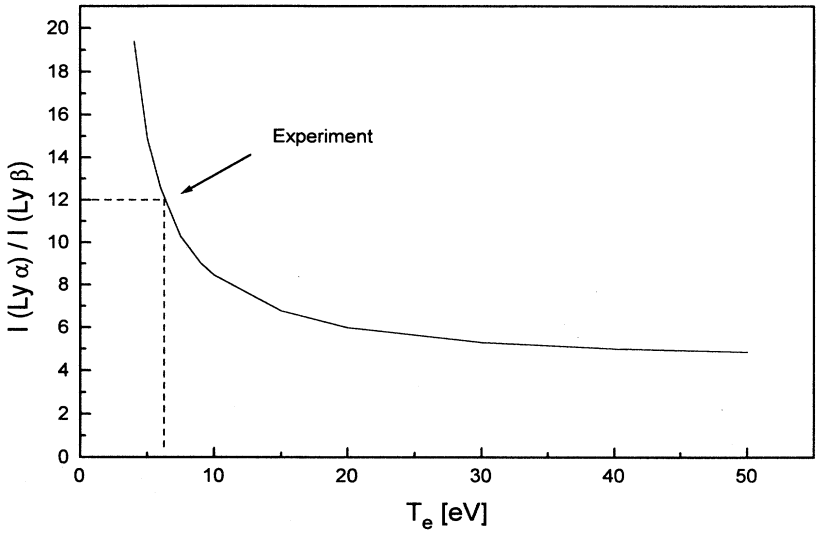

FIG. 11. Effect of initial electron temperature on Lyman-α to Lyman-β ratio of simulated He^+ spectrum. Experimental line ratio is indicated.

that in the simulations the intensity of the N^{4+} $2p$-$4d$ line as compared with that of the N^{4+} $2p$-$3d$ line is too low.

In contrast to helium, varying the electron temperature or assuming a nonzero initial population in the lithiumlike ground state did not result in a better match between experiment and simulations. To bring the simulated spectra into accord with the experimental ones, a mechanism other than three-body recombination must be added to the ion kinetics. We suggest that state-selective charge transfer from molecular nitrogen to the heliumlike ions provides additional input to the $n=4$ level of lithiumlike nitrogen.

In the following this mechanism is discussed in more detail. A charge-transfer reaction according to the equation

$$N^{5+}+N_2 \rightarrow N^{4+,*}+N_2^+ , \tag{4}$$

where the * symbolizes an excited state, selectively populates excited lithiumlike states. Charge transfer is possible only if the reaction is exothermic, i.e., if

$$I_p < E_b , \tag{5}$$

where I_p is the ionization potential of the electron donor and E_b is the binding energy of the populated ionic level.

The ionization potential of N_2 is 15.6 eV. Thus, when the criterion of Eq. (5) is used, state-selective charge transfer is only possible into the $n=4$ shell of lithiumlike nitrogen, the binding energy of which is around 22 eV (depending on the value of the orbital quantum number). The binding energy of the lowest $n=5$ state ($5s$) is 14.4 eV.

To our knowledge, the charge-transfer cross section for the particular system $N^{5+} \rightarrow N_2$ has not been measured. However, the cross section for the reaction $N^{6+} \rightarrow H_2$ is known from work of Afrosimov *et al.* [24] and by Dijkkamp *et al.* [25]. Since the ionization potential of H_2 is quite close to that of N_2, the state selectivity of the two processes should be quite similar, whereas the magnitude

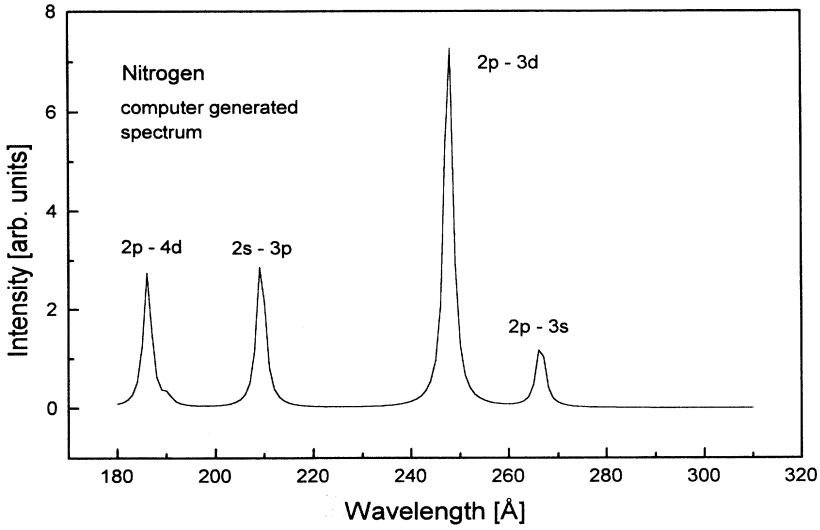

FIG. 12. Simulated time-integrated spectrum of nitrogen under "standard" conditions, i.e., $T_e=20$ eV, $N_e=10^{19}$ cm^{-3}, no ions initially in lithiumlike state.

of the cross section should be higher in the case of N_2 due to the higher number of electrons. Afrosimov *et al.* found for the N^{6+}-H_2 system a total single-electron charge-transfer cross section of 4.5×10^{-15} cm^2 at a relative velocity of 3×10^7 cm/s. Dijkkamp *et al.* found that charge transfer selectively populated the $n=4$ level manifold with a transfer cross section of 3.7×10^{-15} cm^2 at a relative velocity of 5×10^7 cm/s. The data of Dijkkamp *et al.* show that the cross section in this region is fairly independent of the ionic velocity (not so the distribution among orbital quantum numbers). Therefore we may use these measurements to calculate charge-transfer rates and compare them with the recombination rates.

The three-body recombination rate per second may be approximated by [26]

$$R_{3B}=8.75\times10^{-27}q^2(kT_e)^{-9/2}N_e^2 , \quad (6)$$

where q is the ion charge and kT_e is the electron temperature in eV. The radiative recombination rate is given by [26]

$$R_{\rm rad}=2.7\times10^{-13}q^2(kT_e)^{-3/4}N_e . \quad (7)$$

The charge-transfer rate is

$$R_{\rm CT}=\sigma_{\rm CT}v_{\rm rel}N_g , \quad (8)$$

where $\sigma_{\rm CT}$ is the charge-transfer cross-section, $v_{\rm rel}$ the relative velocity of the collision pair, and N_g the number density of gas molecules.

Inserting standard initial conditions of our experiment, i.e., $kT_e=20$ eV, $q=5$, $N_e=10^{19}$ cm^{-3} yields a three-body recombination rate of 1.5×10^8 s^{-1}, whereas the radiative rate is only 7×10^6 s^{-1}. The charge-transfer rate depends on the relative velocity of the collision pair. Inserting a plasma expansion velocity of 2×10^6 cm/s, a cross section $\sigma_{\rm CT}=3.7\times10^{-15}$ cm^2, and a gas density $N_g=10^{18}$ cm^{-3} into Eq. (8) results in a charge-transfer rate of 7.4×10^9 s^{-1}, almost two orders of magnitude higher than the three-body recombination rate.

The true charge-transfer rate will not be as large as estimated above, since the effective densities of both the ions and the neutral gas molecules participating in the charge transfer will be reduced. However, this estimate shows that it is not unreasonable to assume charge transfer as a mechanism which plays a significant role in the kinetics following optical-field ionization.

It should be noted that, in the case of helium, charge transfer into an excited level is not possible, since the reaction would be strongly endothermic. However, the rate of ion depletion may be influenced by charge transfer from neutral helium into the bare nuclei which generates the ground state of hydrogenic helium.

V. GAIN

The simulations predict transient gains on many lines in the ionic spectra. For the $2p$-$3d$ line of lithiumlike nitrogen under standard conditions a gain lasting about 10 ps, with a peak value of 7 cm^{-1}, is calculated.

To search experimentally for amplification, longitudinal and transverse spectra were systematically compared. However, gain on any line to a ground state or quasi-ground-state of lithiumlike nitrogen was not detected. The reason for this negative result may be the time-integrated nature of the spectra, in which emission during the transient amplification is masked by the total emission, which lasts a few nanoseconds.

However, indications of gain on lines between excited states could be observed. In comparing transverse and longitudinal spectra an increase in the emission in the axial direction was consistently observed for several lines in the spectrum, one of which was identified as the $3d$-$5f$ transition of lithiumlike nitrogen with a wavelength of 511.9 Å. In order to confirm the assertion of gain and measure the gain coefficient, a tube was mounted to the end of the nozzle tip. By squeezing the end of the tube a gas jet with long and short dimensions of 800 and 400 μm could be generated. In Fig. 13 a transverse spectrum is compared with longitudinal spectra taken along the short and long dimensions of the gas jet. The f number of the spectrograph was low enough to record the total emission in the transverse direction. It is seen that in the longitudinal spectrum along the 400 μm dimension the emission of N^{4+} $3d$-$5f$ is increased relatively to the $3p$-$5d$ line. Along the 800 μm dimension the $3d$-$5f$ emission shows a further, nonlinear increase. The $3p$-$5d$ line is—according to the simulations—also temporarily inverted, but exhibits considerably lower gain. Lorentzians are fitted to the various lines to correct for the effect of adjacent transitions. By fitting the data to the Linford formula [27] a gain coefficient of 28 ± 9 cm^{-1} is determined for the $3d$-$5f$ line. A similar gain value is calculated for another, boronlike line in the spectrum, i.e., N^{2+} $2s2p^2$-$2s2p3d$ at 472.4 Å. A Linford plot for both of these lines is shown in Fig. 14.

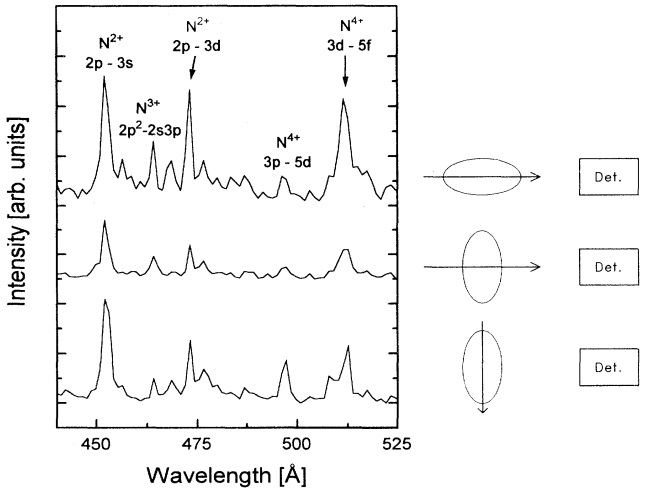

FIG. 13. Comparison of nitrogen spectra in the region of transitions between excited lithiumlike states. The three spectra are obtained using a gas jet with an oval cross section of 400 and 800 μm extension, respectively. A transverse spectrum and two longitudinal spectra (along the short and long dimensions of the gas jet) are displayed, as indicated by the symbols alongside each spectrum. Gain lines are indicated by arrows.

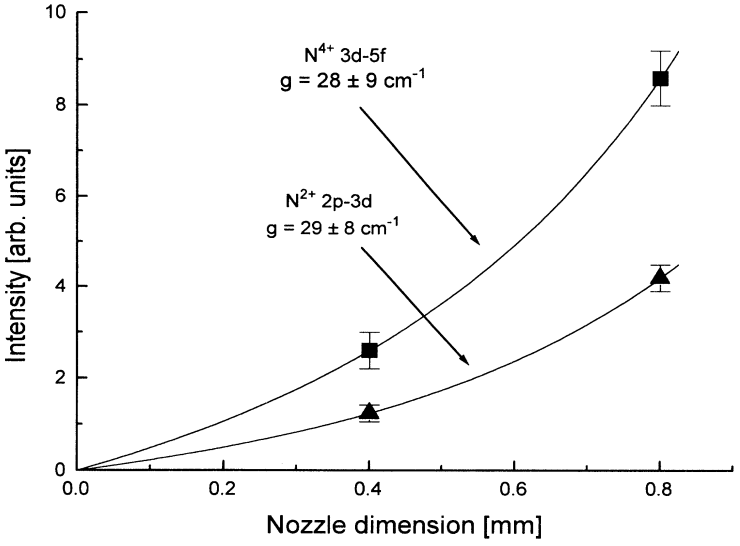

FIG. 14. Linford plot for N^{4+} and N^{2+} gain lines. The data for N^{2+} are scaled down by a factor of 2 to avoid overlap of the curves.

A number of computer runs were performed to investigate the conditions of lasing on the N^{4+} $3d$-$5f$ transition. The simulations predict this line to be temporarily inverted in a wide range of electron densities and temperatures. For standard conditions ($T_e=20$ eV, $N_e=10^{19}$ cm^{-3}) a gain lasting 6 ps with a peak value of about 10 cm^{-1} is calculated. A gain coefficient close to that experimentally observed is obtained if the initial electron temperature is reduced to 10 eV. For this condition the peak gain coefficient is 28 cm^{-1} and the gain lasts about 4 ps (see Fig. 15).

The gain values predicted by the simulations rest on the assumption that the initial ion temperature is determined merely by momentum transfer from the stripped electrons, which leads to initial ion temperatures of only a fraction of an eV. In contrast to this, recent measurements for helium yielded an initial ion temperature of about 3 eV, which was attributed to ion-ion collisions in the laser field [22]. Since the applied intensities in these investigations were a factor of about 10 higher than ours, the ion temperature in our experiment may still be below 1 eV. However, for molecules the situation is more complicated since additional ion heating may result from a "Coulomb explosion" [28,29]. More investigations of optical-field ionization, especially in molecules, are needed in order to clarify the role of the various physical mechanisms affecting the ion temperature.

It remains to explain the unexpectedly high gain observed in this and similar experiments [30,31]. One explanation is that different electron populations with different electron temperatures exist, which have not yet relaxed to a single Maxwellian distribution. However, this possibility seems somewhat esoteric, considering the electron-electron self-relaxation time at an electron density of 10^{19} cm^{-3}, which is calculated to be about 0.5 ps [32].

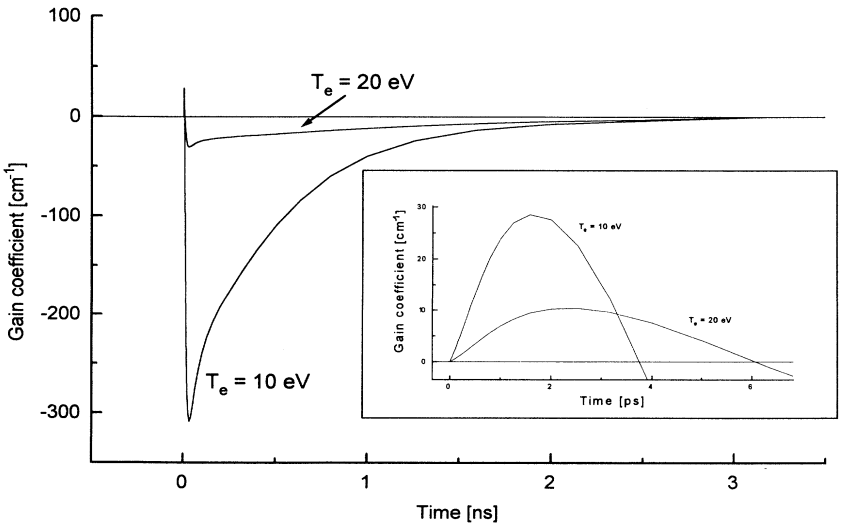

FIG. 15. Time-dependent gain coefficient for N^{4+} $3d$-$5f$ transition at 511.9 Å. Numerical results for initial electron temperatures of 20 and 10 eV are shown. Inset shows evolution of the gain coefficient on an expanded time scale.

Another explanation has been put forward by Eder *et al.* [31] in connection with their observation that the time dependence of the Lyman-α emission in H-like Li after field ionization was consistent with an electron temperature significantly below that given by ATI heating. They suggest that the removal of the first electron should be treated as multiphoton ionization rather than field ionization. In this case the first electron would be ejected with rather low energy, which would reduce the temperature of the resulting electron population. In the case of nitrogen, however, the lowering of the final electron temperature would not be dramatic since this effect applies only to one out of the ten electrons removed from the nitrogen molecule. Another possibility would be that the fastest electrons escape from the plasma, thus leaving a colder electron gas behind.

VI. CONCLUSION

By focusing terawatt Ti:sapphire laser pulses into a gas jet of He, N_2, CO_2, O_2, Ar, and SF_6 xuv emission on lines of hydrogenic helium, lithiumlike nitrogen, carbon, and oxygen as well as of sodiumlike argon and sulfur could be generated. This result is in accord with the classical barrier suppression model, which predicts the corresponding parent ions to be readily generated at the intensities of up to 5×10^{16} W/cm^2 used in the experiment. A striking dissimilarity between the helium spectra and the spectra of the other gases was observed with regard to the relative strength of the first and second resonance lines. This finding is partially explained by the fact that the predicted electron temperature in helium is close to the ionization potential of hydrogenic helium, whereas in the other gases it is considerably lower than the ionization potential of the relevant ionization stage. Simulations reveal that the helium spectra can be explained as being due either to collisional excitation from the hydrogenic ground state or to a low electron temperature. The nitrogen spectra can only be approximately reproduced by the simulations, with the anomalously high emission on the $2p$-$4d$ line of lithiumlike nitrogen suggesting the assumption of a different process populating the $n=4$ level. Charge transfer with the neutral nitrogen is discussed as a possibility. Finally, evidence of gain on the $3d$-$5f$ transition in lithiumlike nitrogen at a wavelength of 511.9 Å has been obtained. The simulations predict a gain value as experimentally observed if the initial electron temperature is assumed to be considerably below the one given by ATI heating (10 instead of 20 eV) and for an initial ion temperature as given by recoil from the ejected electrons.

ACKNOWLEDGMENTS

Valuable discussions with D. Eder are gratefully acknowledged. We thank A. Persson for operating the laser and L. Engström for the loan of the spectrometer. Thanks are due to G. Pretzler for performing the Abel inversion. This work was supported by the Swedish National Science Research Council and was performed within the framework of the European X-Ray Laser Network.

[1] L.V. Keldysh, Zh. Eksp. Teor. Fiz. **47**, 1945 (1964) [Sov. Phys. JETP **20**, 1307 (1965)].
[2] A. L'Huiller, L. A. Lompré, G. Mainfray, and C. Manus, Phys. Rev. Lett. **48**, 1814 (1982).
[3] T. S. Luk, H. Pummer, K. Boyer, M. Shahidi, H. Egger, and C. K. Rhodes, Phys. Rev. Lett. **51**, 110 (1983).
[4] P. B. Corkum, N. H. Burnett, and F. Brunel, Phys. Rev. Lett. **62**, 1259 (1989).
[5] M. D. Perry, A. Szoke, O. L. Landen, and E. M. Campbell, Phys. Rev. Lett. **60**, 1270 (1988).
[6] N. H. Burnett and P. B. Corkum, J. Opt. Soc. Am. B **6**, 1195 (1989).
[7] J. Peyraud and N. Peyraud, J. Appl. Phys. **43**, 2993 (1972).
[8] N. H. Burnett and G. D. Enright, IEEE J. Quantum Electron. **26**, 1797 (1990).
[9] P. Amendt, D. C. Eder, and S. C. Wilks, Phys. Rev. Lett. **66**, 2589 (1991).
[10] S. Augst, D. Strickland, D. D. Meyerhofer, S. L. Chin, and J. H. Eberly, Phys. Rev. Lett. **63**, 2212 (1989).
[11] S. Augst, D. D. Meyerhofer, D. Strickland, and S. L. Chin, J. Opt. Soc. Am. B **8**, 858 (1991).
[12] B. M. Penetrante and J. N. Bardsley, Phys. Rev. A **43**, 3100 (1991).
[13] S. Svanberg, J. Larsson, A. Persson, and C.-G. Wahlström, Phys. Scr. **49**, 187 (1994).
[14] G. W. Faris and H. M. Hertz, Appl. Opt. **28**, 4662 (1989).
[15] R. L. Kelly, in *Atomic and Ionic Spectrum Lines Below 2000 Angstroms: Hydrogen through Krypton,* special issue of J. Phys. Chem. Ref. Data **16**, Suppl. 1 (1987).
[16] W. L. Wiese, M. W. Smith, and B. M. Glennon, *Atomic Transition Probabilities,* Natl. Bur. Stand. Ref. Data Ser., Natl. Bur. Stand. (U.S.) Circ. No. 4 (U.S. GPO, Washington, DC, 1966).
[17] A. Lindgard and S. E. Nielsen, At. Data Nucl. Data Tables **19**, 533 (1977).
[18] G. Pretzler, H. Jäger, T. Neger, H. Philipp, and J. Woisetschläger, Z. Naturforsch. **47a**, 955 (1992).
[19] M. Dunne, T. Afshar-Rad, J. Edwards, A. J. MacKinnon, S. M. Viana, O. Willi, and G. Pert, Phys. Rev. Lett. **72**, 1024 (1994).
[20] N. B. Delone and V. P. Krainov, J. Opt. Soc. Am. B **8**, 1207 (1991).
[21] A. A. Offenberger, W. Blyth, A. E. Dangor, A. Djaoui, M. H. Key, Z. Najmudin, and J. S. Wark, Phys. Rev. Lett. **71**, 3983 (1993).
[22] T. E. Glover, T. D. Donnelly, E. A. Lipman, A. Sullivan, and R. W. Falcone, Phys. Rev. Lett. **73**, 78 (1994).
[23] R. A. London and M. D. Rosen, Phys. Fluids **29**, 3813 (1986).
[24] V. V. Afrosimov, A. A. Basalaev, E. D. Donets, and N. N. Panov, Pis'ma Zh. Eksp. Teor. Fiz. **31**, 635 (1980) [JETP Lett. **31**, 600 (1980)].

[25] D. Dijkkamp, Yu. S. Gordeev, A. Brazuk, A. G. Drentje, and F. J. de Heer, J. Phys. B: At. Mol. Phys. **18**, 737 (1985).
[26] Ya. B. Zeldovich and Yu. P. Raizer, *Physics of Shock Waves and High-Temperature Hydrodynamic Phenomena* (Academic, New York, 1966), p. 407.
[27] G. J. Linford, E. R. Peressini, W. R. Sooy, and M. L. Spaeth, Appl. Opt. **13**, 397 (1974).
[28] K. Boyer, T. S. Luk, J. C. Solem, and C. K. Rhodes, Phys. Rev. A **39**, 1186 (1989).
[29] C. Cornaggia, J. Lavancier, D. Normand, J. Morellec, and H. X. Liu, Phys. Rev. A **42**, 5464 (1990).
[30] Y. Nagata, K. Midorikawa, S. Kubodera, M. Obara, H. Tashiro, and K. Toyoda, Phys. Rev. Lett. **71**, 3774 (1993).
[31] D. C. Eder, P. Amendt, L. B. DaSilva, R. London, B. J. MacGowan, D. L. Matthews, B. M. Penetrante, M. D. Rosen, and S. C. Wilks, Phys. Plasmas **1**, 1744 (1994).
[32] L. Spitzer, Jr., *Physics of Fully Ionized Gases* (Interscience, New York, 1956), p. 78.